

**Piotr Mackiewicz**

PhD, Eng., Prof. PWR  
Wrocław University of Science and Technology,  
Department of Roads, Bridges, Railways, and Airports  
piotr.mackiewicz@pwr.edu.pl  
ORCID: 0000-0002-3170-6415

**Antoni Szydło**

Prof., PhD, Eng.,  
Wrocław University of Science and Technology,  
Department of Roads, Bridges, Railways, and Airports  
antoni.szydlo@pwr.edu.pl  
ORCID: 0000-0002-3363-9391

DOI: 10.35117/A\_ENG\_25\_11\_08

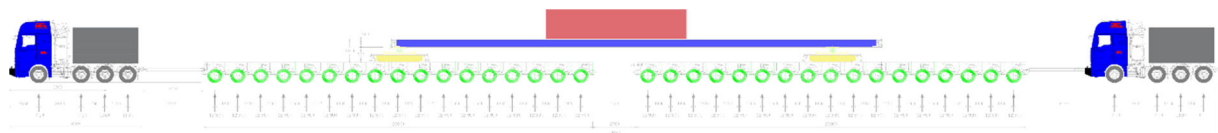
**The impact of the aggressiveness of a combination of vehicles and low-bed trailers for the transport of oversize loads on road surfaces**

**Abstract:** This article assesses the load-bearing capacity of road surfaces as a result of the impact of a combination of vehicles and low-bed trailers transporting oversized loads. The analysis was conducted using the example of transporting TBM shield components for tunneling on the S19 expressway in Babica. The route begins in Opole and ends on the S19 expressway in Babica.

**Keywords:** Flexible pavement; Rigid pavement; Standard axle; Overload; Fatigue life

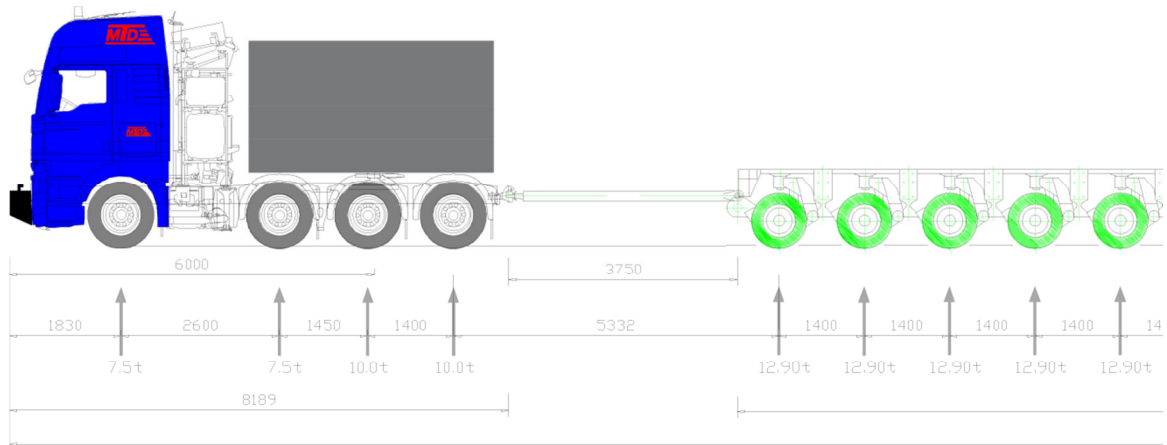
**Description and Characteristics of the Transport Set**

The transport set consists of a pulling vehicle (first vehicle – the tractor), two low bed transport trailers, and a pushing–braking vehicle (last vehicle – the pusher). Figure 1 shows a schematic of the transport set.

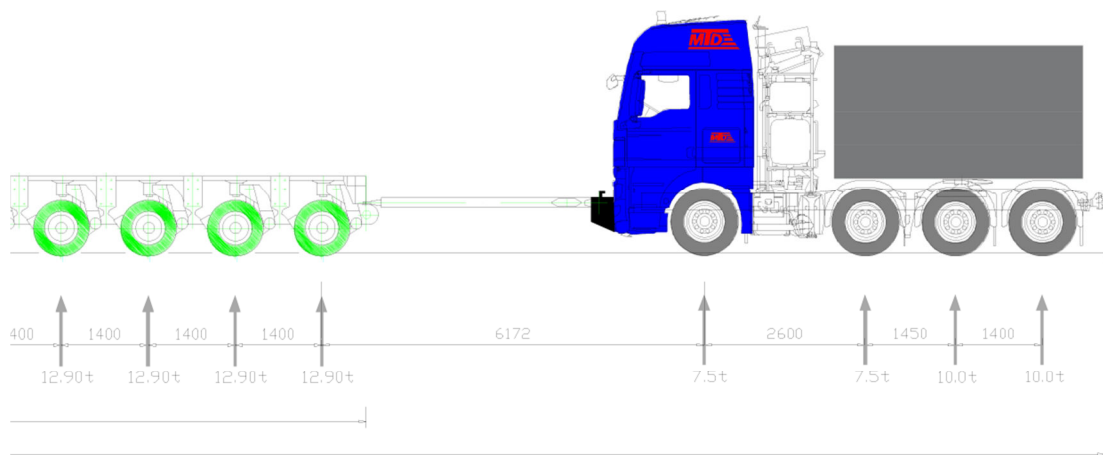


1. Schematic diagram of the transport set

The tractor has 4 axles, each trailer has 17 axles, and the pusher also has 4 axles. Figures 2 and 3 show the tractor and pusher with parts of the trailer.

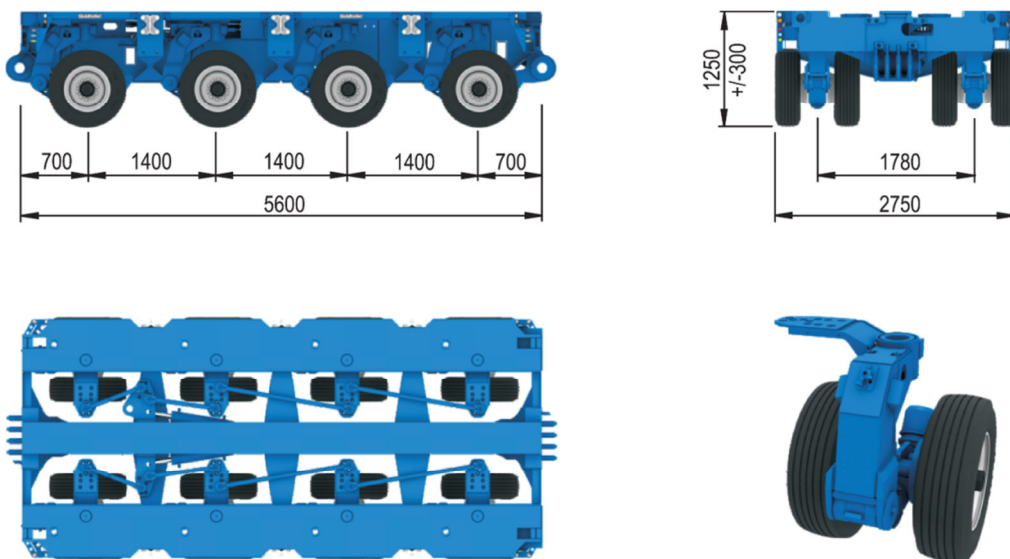


2. Tractor with a fragment of the trailer



3. Pusher with a fragment of the trailer

Figures 2 and 3 also present axle loads and axle spacing. In the tractor and pusher, the maximum axle load is 100 kN, with spacing of 1.4 m and 1.45 m. The 100 kN axles in these vehicles have twin wheels. In the trailers, the maximum axle load is 129 kN, with spacing of 1.4 m. Figure 4 shows detailed trailer dimensions.

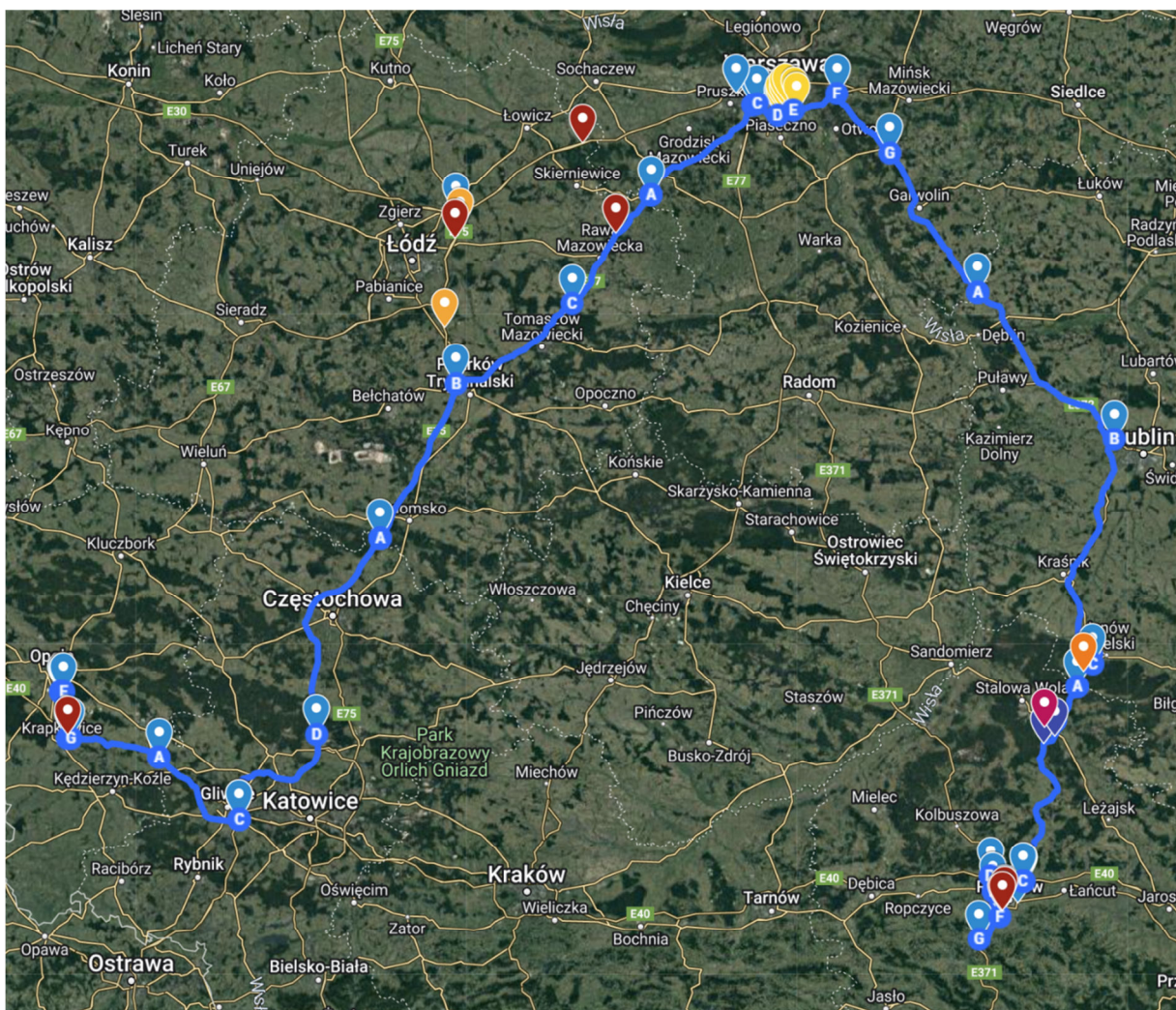


4. Detailed dimensions of the trailer

The distance between the centers of twin wheels is 1.78 m. The lateral spacing of twin wheels is 0.705 m. The distance between the inner wheels of the twin set is 0.81 m. The unit pressure exerted by a wheel on the pavement is 0.9 MPa. These parameters—axle loads, axle spacing, and wheel spacing—were used to develop the load model for the transport set acting on the pavement.

### Transport Route

The route begins at the Opole Port – Metalchem and ends in Babica on the S19 expressway. The total length is approximately 745 km. The planned route includes the following roads: DW423, A4, A1, S8, S2, S17, S19, DK19, S19, A4, A19, A4, S19, DK9, DK19, DW988. These roads include various pavement types constructed in asphalt and concrete technologies. Based on data provided by the client, the pavement types on individual sections were identified. Figure 5 shows the planned route.

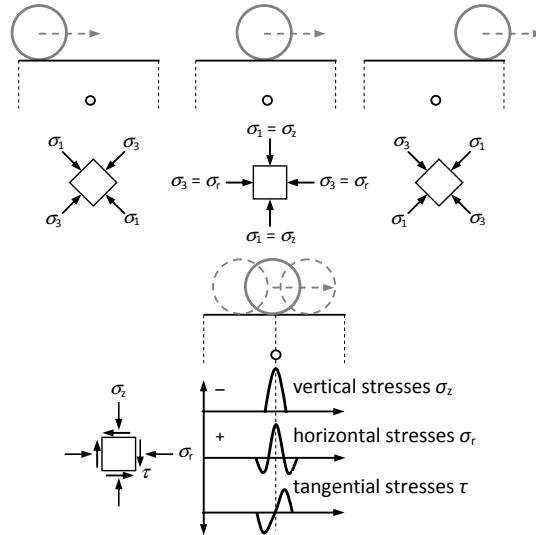


5. Transport route of the set

### Pavement Load Models

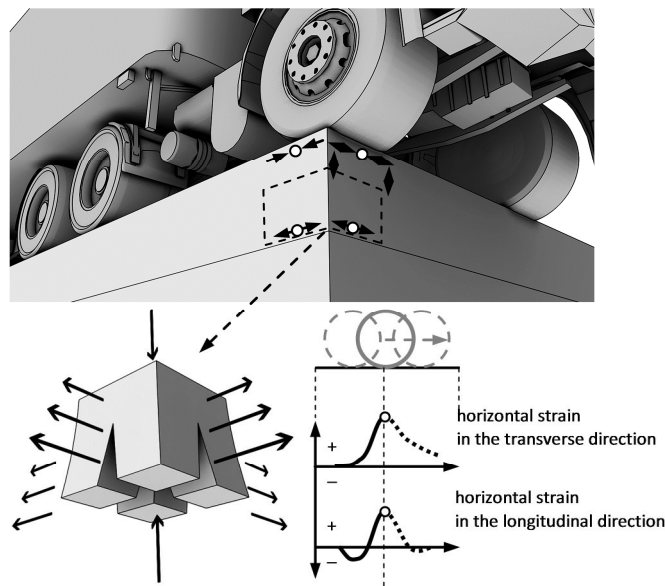
To estimate the impact of the transport set on pavements along the route and the potential loss of pavement durability, several models were developed. The first stage involved creating a load model for the transport set. The analysis was carried out using a numerical model based on an elastic half space.

A key factor in pavement analysis is the way loads are transferred through wheels and the relative positioning of axles. As wheels pass over the pavement, a complex stress state develops in the lower pavement layers (Figure 6), including vertical, horizontal, and shear stresses causing compression and tension.



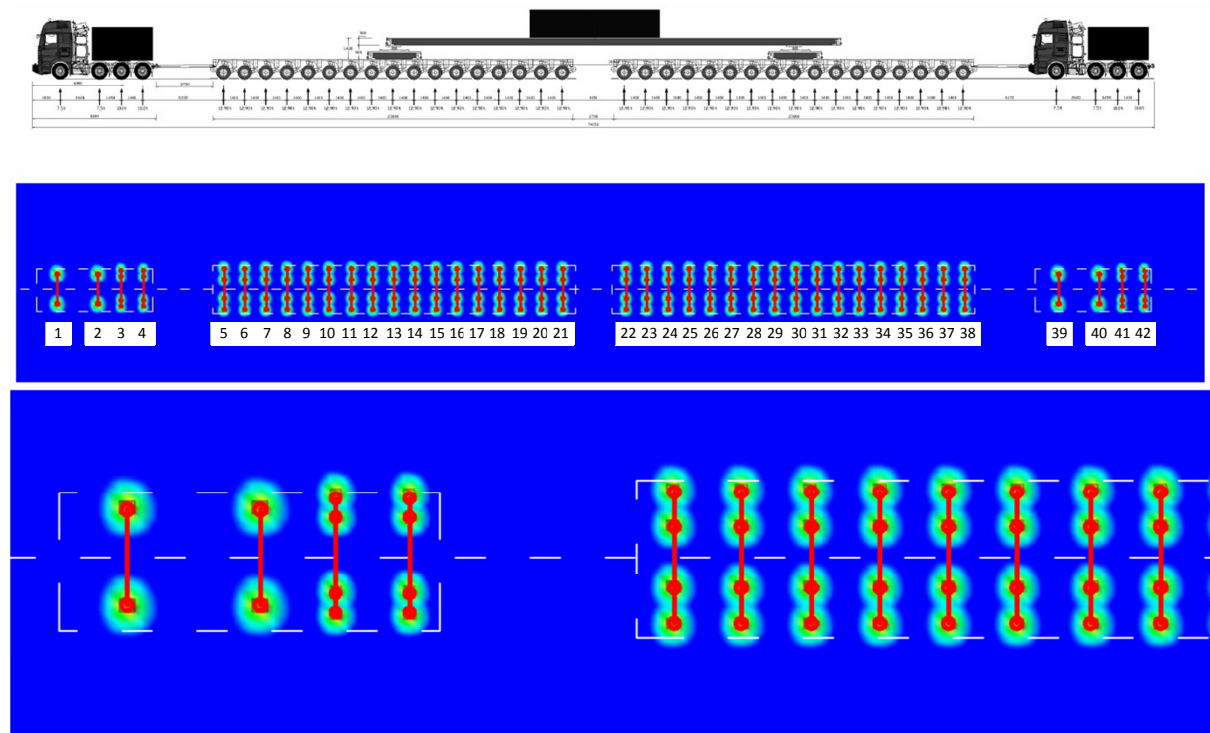
6. Change in stress distribution during wheel passage

The relative position of axles and wheel types (single or twin) significantly affects deformation and stress distribution (Figure 7).



7. Typical strain distribution in pavement under load

Preliminary calculations indicated that the entire set and full axle configuration must be considered, despite large distances between axles (2.6 m for vehicles and 1.4 m for trailers). Depending on pavement stiffness, stresses and deformations at different depths may cancel or accumulate due to superposition. Figure 8 shows the load model used in numerical analyses.



8. Load model

The model includes axle and wheel configurations within each axle. The adopted load parameters for individual components of the transport set are presented in Table 1.

Tab. 1. Load parameters for individual elements of the transport set

<b>tractor</b>					
	Axle load [kN]	Wheel load [kN]	Load footprint radius [m]	Axle spacing in cross-section [m]	Wheel spacing between twin wheels [m]
Axis 1	75	37.5	0.118	2	-
Axis 2	75	37.5	0.118	2	-
Axis 3	100	25	0.094	2	0.309
Axis 4	100	25	0.094	2	0.309
<b>trailer 1</b>					
Each of the 17 axes	129	32.25	0.107	1.78	0.705
<b>trailer 2</b>					
Each of the 17 axes	129	32.25	0.107	1.78	0.705
<b>pusher</b>					
Axis 1	75	37.5	0.118	2	-
Axis 2	75	37.5	0.118	2	-
Axis 3	100	25	0.094	2	0.309
Axis 4	100	25	0.094	2	0.309

Additionally, a separate model of a standard 115 kN axle was considered, modeled as a single axle with twin wheels (Table 2).

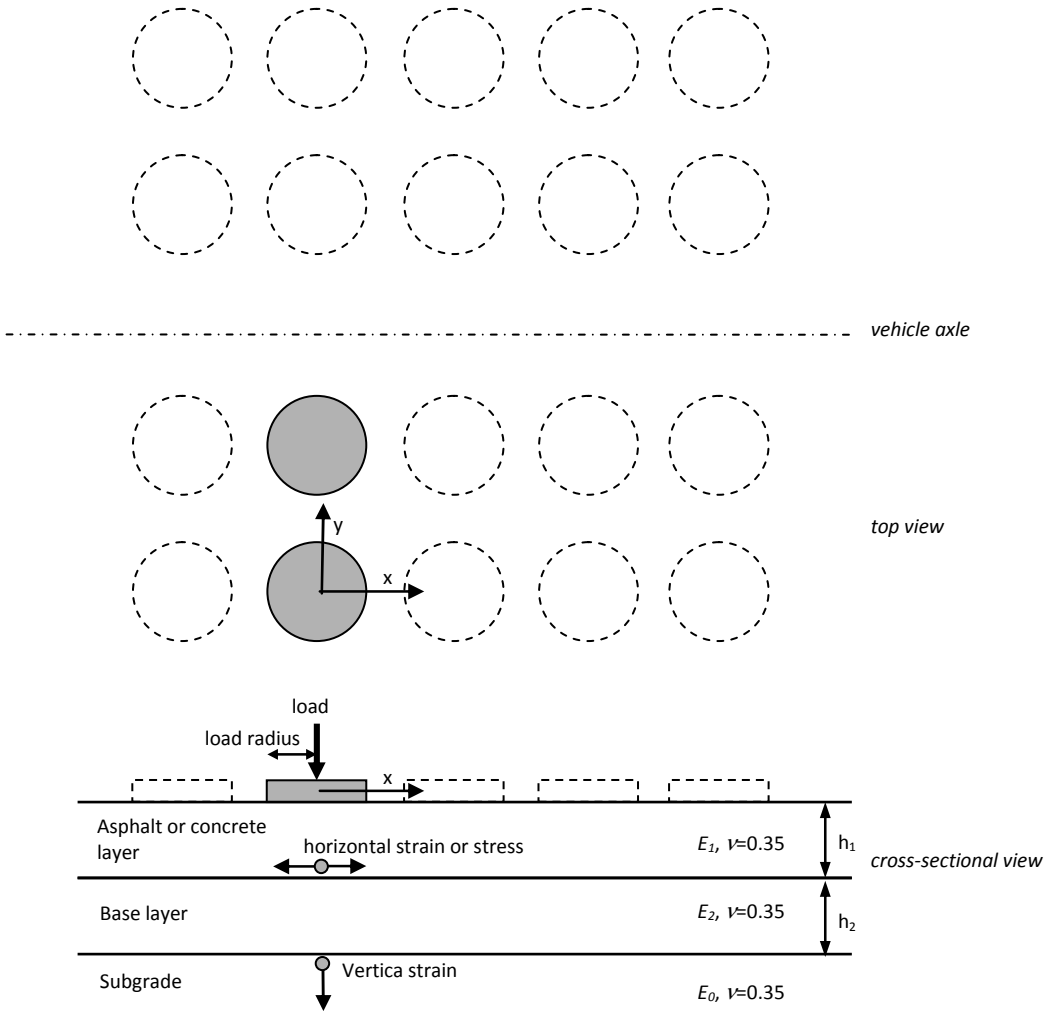
**Tab. 2.** Load parameters for the standard axle

Standard axle					
	Axle load [kN]	Wheel load [kN]	Load footprint radius [m]	Axle spacing [m]	Wheel spacing between twin wheels [m]
Axis	115	28.75	0.103	2	0.309

**Pavements and Pavement Models along the Route**

In the second stage, pavement models were developed based on identified pavement structures provided by the client. The adopted pavement system consists of the following layers (Fig. 9):

- asphalt layers or concrete slab,
- base layer,
- subgrade layer.



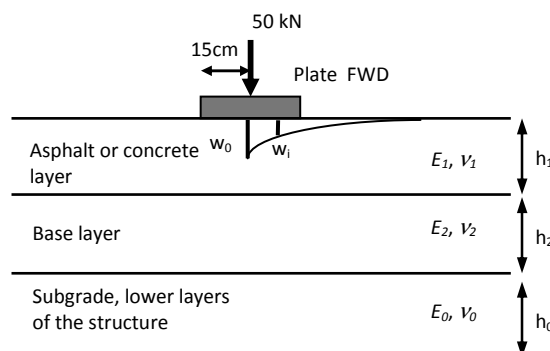
**9. Layered pavement model**

The analyses considered the entire axle configuration of the transport set. In calculations based on the layered elastic half-space model, tensile strains at the bottom of asphalt layers or tensile stresses at the bottom of the concrete slab, as well as vertical strains

in the subgrade, were identified. These values were subsequently used to assess pavement durability. Additionally, values in both the x- and y-directions were considered, as wheel configurations make directional effects non-uniform.

Model parameters were determined based on the identification of pavement moduli using deflection basin parameters provided by the client, obtained from DSN diagnostics. Deflections were measured using an FWD device, and the SCI300 parameter (difference between maximum deflection and deflection at 0.3 m from the load axis) was used.

For newly constructed sections without DSN diagnostics, design parameters from mechanistic pavement design methods were adopted. Figure 10 presents the parameter identification model.



10. Computational model for modulus identification

The pavement structure consists of three layers:

- layer of thickness  $h_1$  representing asphalt layers or concrete slab,
- layer of thickness  $h_2$  representing the base,
- layer of thickness  $h_0$  representing the equivalent subgrade.

Calculations were performed using the CZUG program developed by the author [1]. The identification process yields elastic moduli ( $E_i$ ) of individual layers. Poisson's ratios had no significant influence on the resulting moduli.

Table 3 presents selected asphalt and concrete pavement structures along the route and their parameters in three-layer models.

Tab. 3. Characteristics of selected pavement structures along the route

#### DW423 Opole, park przemysłowy METALCHEM

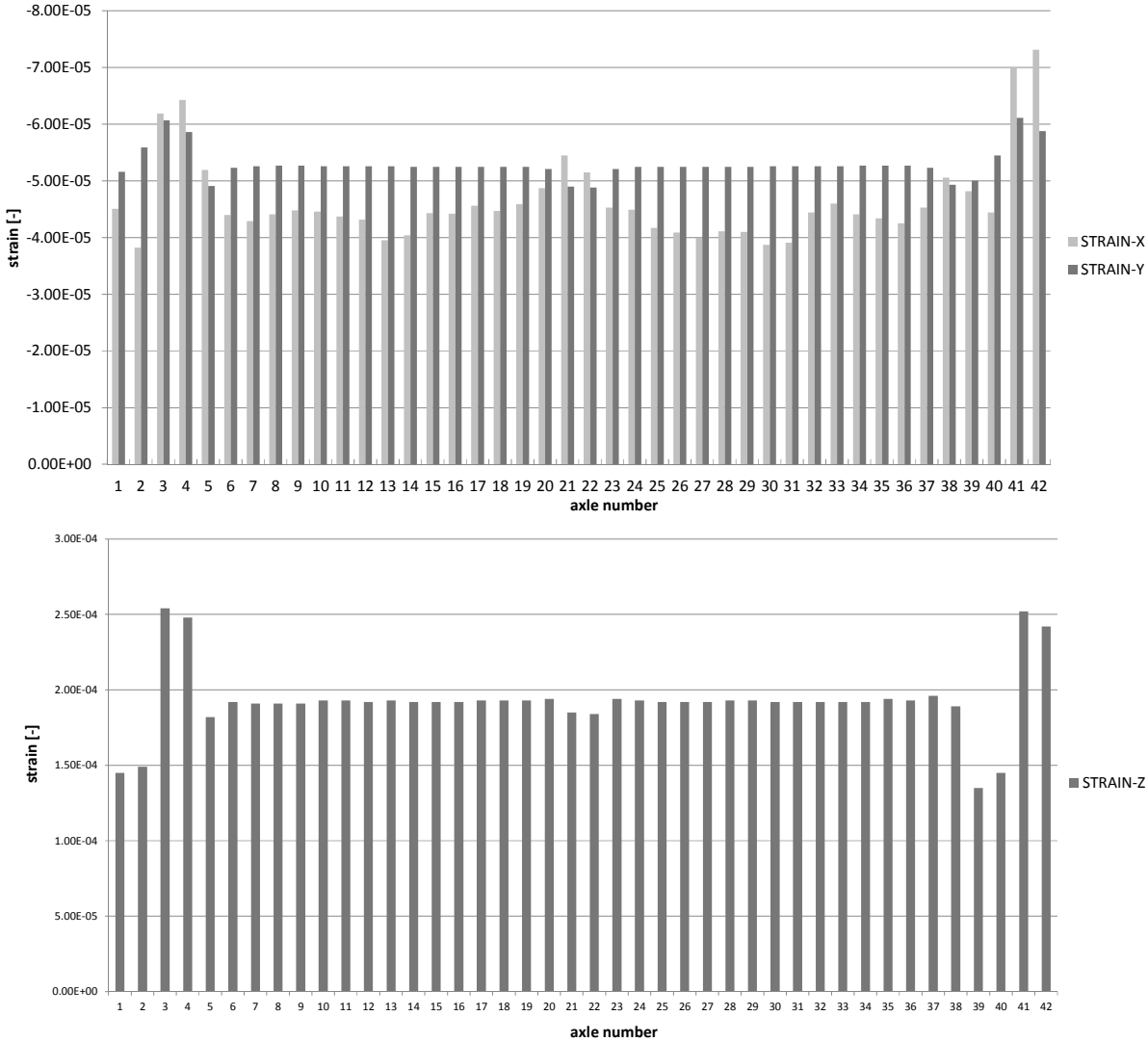
Layer	Thickness [cm]	Layer thickness in the model [cm]	Model parameters [MPa]
MMA SMA11	4	18	13 000
MMA AC16W PMB	5		
ACWMS	9		
MNZ 0/31.5	20	20	400
MZSH/Subgrade	20		120

#### A1 Pyrzowice - Bełchatów (Piotrków Trybunalski)

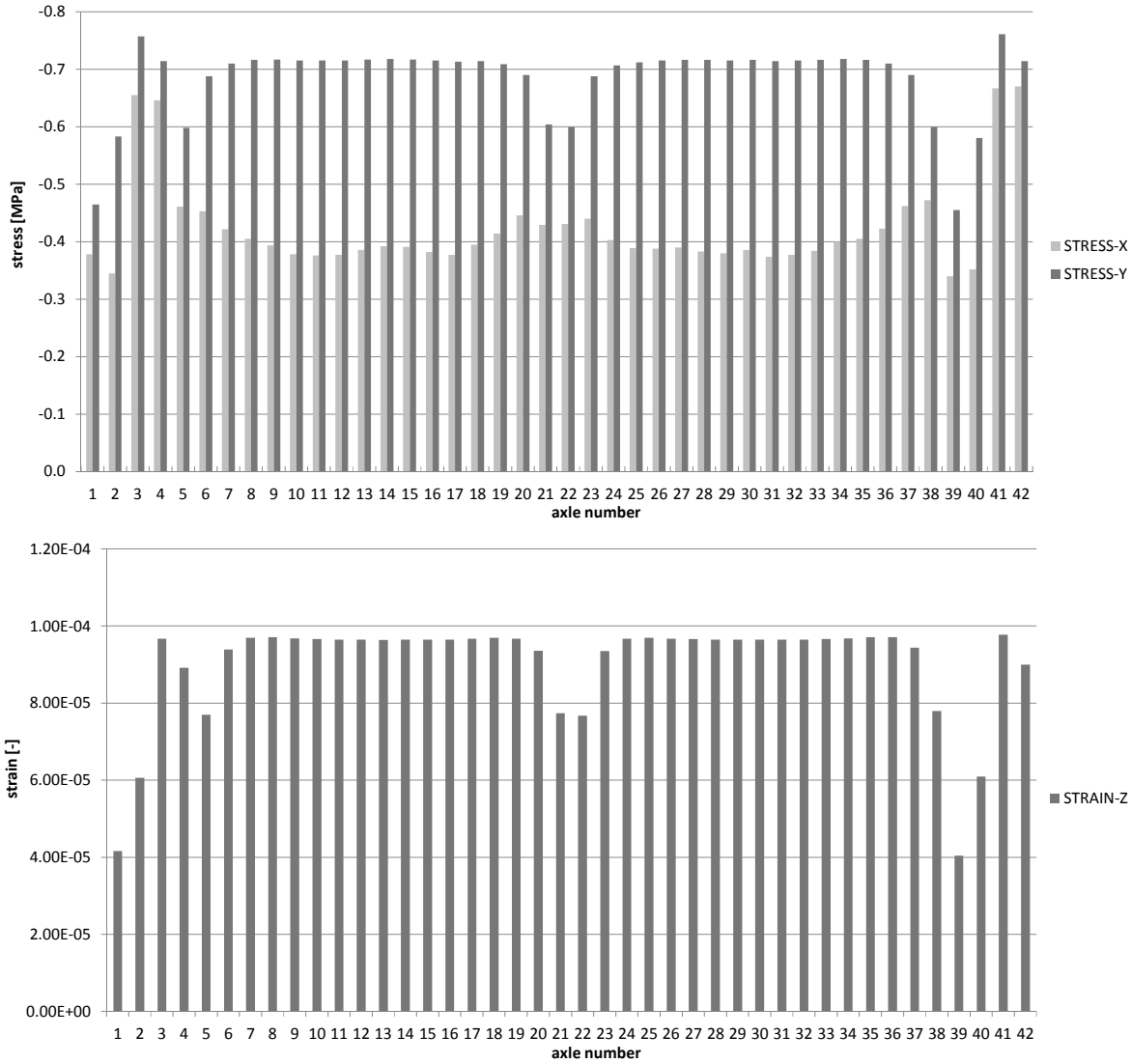
Layer	Thickness [cm]	Layer thickness in the model [cm]	Model parameters [MPa]
Concrete slab	29	29	35 000
MZSH C8/10	20	20	2 000
Subgrade			120

### Results of Stress and Strain Calculations

Based on pavement model calculations, values of stresses and strains were obtained. Example results for selected pavement types are shown in Figures 11 and 12.



11. Results for DW423 Opole, METALCHEM industrial park



12. Results for A1 Pyrzowice – Bełchatów (Piotrków Trybunalski)

Different values of strains were obtained for different pavement types and axles. It should be noted that strain or stress values are higher in the Y direction (transverse to vehicle travel). The highest values occur for outer axles and for axles in the tractor and pusher (100 kN axles). These axles have closely spaced twin wheels, resulting in high contact pressures over a small area. In trailers, although axle loads are higher, they are distributed over a larger area and twin wheels are spaced further apart, preventing strain accumulation.

Pavement Durability Results

Fatigue durability is defined as the allowable number of repeated stress or strain cycles a pavement can withstand before failure. In pavement analysis, durability corresponds to the number of axles the pavement can carry before reaching a critical condition. Depending on pavement type, the critical condition may be cracking or excessive deformation.

In this study, the Asphalt Institute criterion was used for asphalt pavements, while for concrete pavements the criterion from the Catalogue of Typical Rigid Pavement Structures was applied [2]. For subgrade durability, the Asphalt Institute structural deformation criterion was adopted. The general fatigue criterion is expressed as [4], [5]:

$$N_f = Ck_1 \left( \frac{1}{\varepsilon_t} \right)^{k_2} \left( \frac{1}{E} \right)^{k_3} \quad (1)$$

where:

- $N_f$  – number of loads to cause fatigue cracking, [-],
- $\varepsilon_t$  – tensile strain at the critical point of the cross-section, [-],
- $E$  – stiffness modulus of MMA, [MPa],
- $C$  – coefficient dependent on MMA properties, [-],
- $k_1, k_2, k_3$  – regression coefficients, [-].

For the Asphalt Institute criterion, the following relationship is used:

$$N_f = 18.4 \cdot 10^{4.84(V_b/(V_a+V_b)-0.69)} \cdot 6.167(10^{-5}) \cdot \left( \frac{1}{\varepsilon_t} \right)^{3.291} \left( \frac{1}{E} \right)^{0.854} \quad (2)$$

where:

- $V_a$  – void content [%], assumed value 7%,
- $V_b$  – sphalt volume content [%], assumed value 9%.

The pavement (subgrade) structural deformation criterion allows for determining the durability of a structure up to a critical structural deformation of 12.5 mm based on the relationship between the allowable number of repeated loads and the vertical deformation of the subgrade. It is defined by the general relationship:

$$\varepsilon_p = k \cdot (1/N)^m \quad (3)$$

where:

- $\varepsilon_p$  – vertical deformation on the subsoil surface [-],
- $k, m$  – experimental coefficients depending on the type of criterion,  $1.05 \times 10^{-02}$ , 0.223,
- $N$  – number of permissible loads until critical structural deformation occurs.

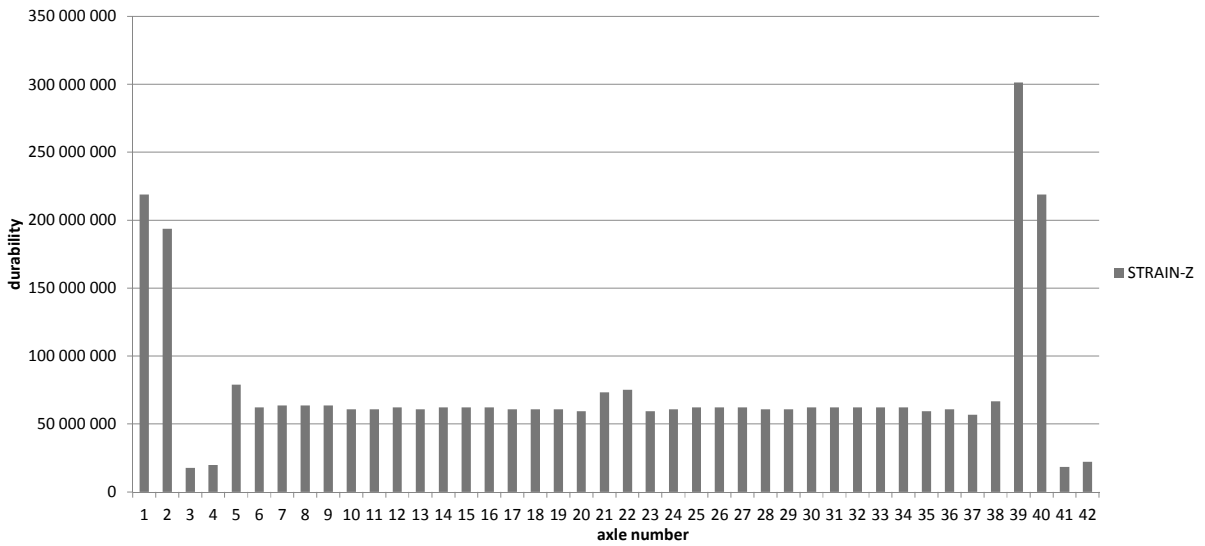
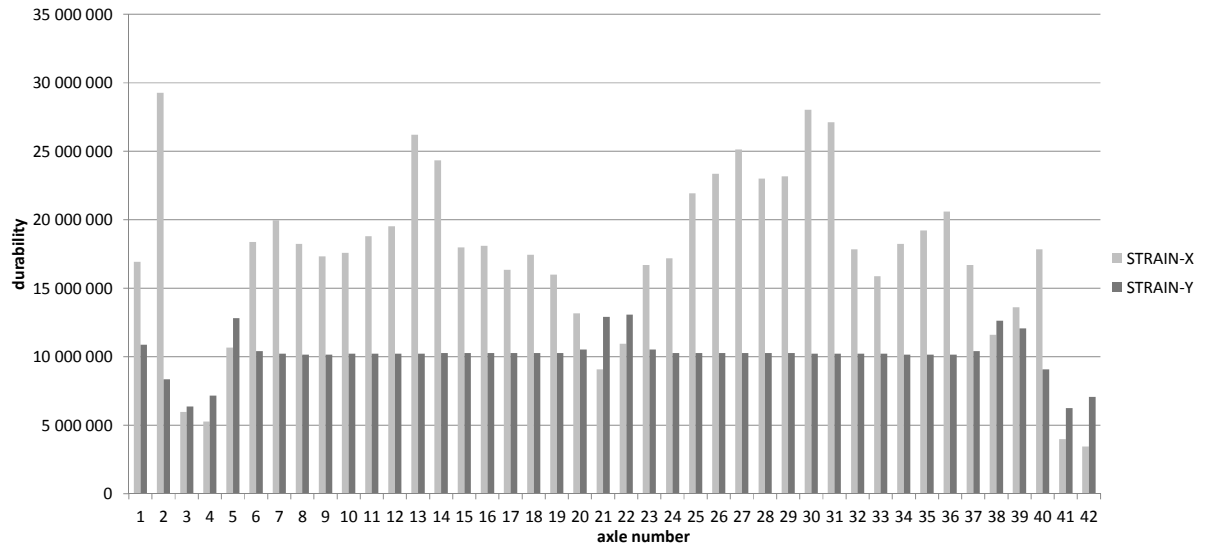
The durability analysis of the concrete pavement (slab) was performed using the relationship defining the allowable strength of the concrete slab as a function of the number of loads (6).

$$F(\sigma_{dop}) = R_{zg} \cdot (1 - 0.078 \cdot \log N) \quad (4)$$

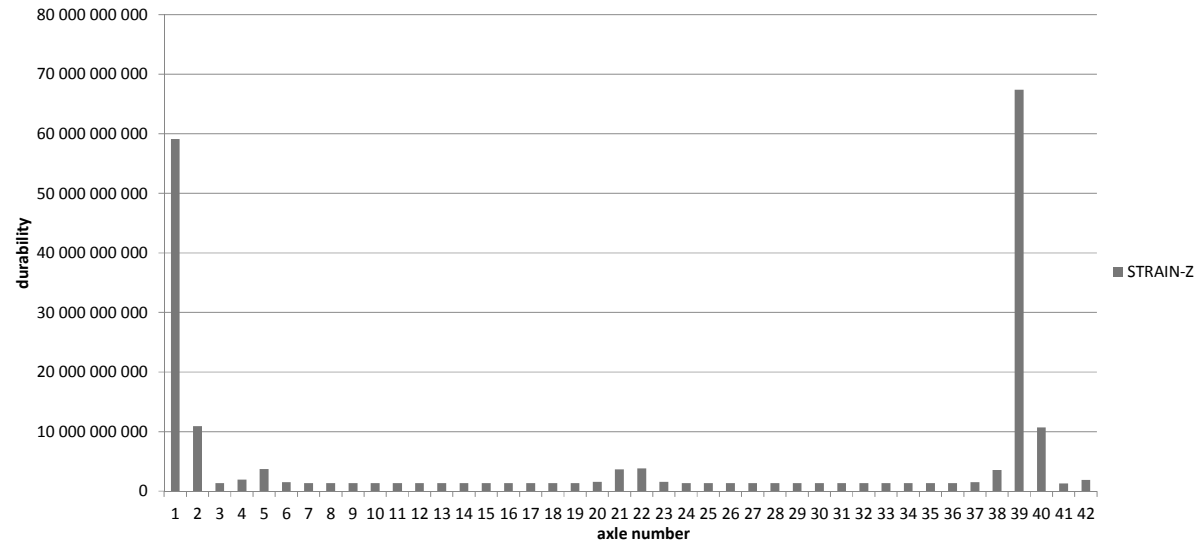
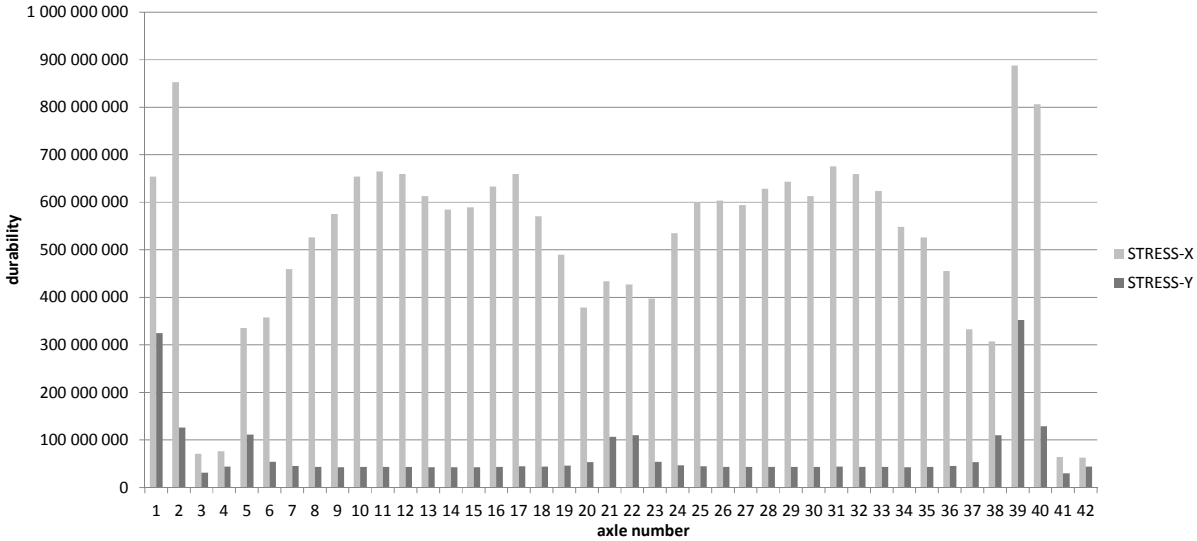
where:

- $R_{zg}$  – flexural tensile strength (assumed 5.5 MPa),
- $N$  – number of repeated loads,
- $F(\sigma_{dop})$  – stress function in the concrete slab due to load and temperature,
- $F(\sigma_{dop}) = \gamma_m \cdot [\gamma_p \cdot (n \cdot \sigma_p) \cdot \gamma_t \cdot (n \cdot \sigma_t)]$ ,  $\gamma_m, \gamma_p, \gamma_t$  – coefficients: material (1.2), load (1.2), temperature (1.2),  $\sigma_p, \sigma_t$  – stresses due to load [MPa] and temperature [MPa],  $n$  – doweling coefficient (0.8).

The stress durability calculations took into account that the load acts on the edge of the plates (unfavorable variant) and there was a temperature gradient, the value of which was adopted according to KTKNSz. Durability results for selected road sections are shown in Figures 13 and 14.



13. Results for DW423 Opole, METALCHEM industrial park



14. Results for A1 Pyrzowice – Bełchatów (Piotrków Trybunalski)

Based on the calculations, various fatigue life values were obtained. These depend on previously obtained values of deformation and stresses occurring in the asphalt layers or concrete slab, as well as in the subgrade.

In the next stage of the analysis, to reliably assess the impact of pavement degradation resulting from the transport unit's passage, the fatigue damage caused to the pavement was analyzed, defined as the sum of the values 1/N<sub>i</sub>.

N<sub>i</sub> represents the fatigue life calculated for the next i<sup>th</sup> axle in the transport unit. Fatigue damage was analyzed for the X and Y directions, as well as the impact on the subgrade Z. To determine the magnitude of the impact of the transport unit relative to a standard 115 kN axle, the aggressiveness of the transport unit was determined as the ratio of the damage to the transport unit and the damage to the 115 kN axle. The aggressiveness coefficient value allows us to determine the number of standard axles that would cause fatigue damage equal to the passage of the transport unit (tractor + 17-wheel trailer + 17-wheel trailer + pusher). For example, an aggressiveness factor of 12 means that the passage of one transport unit causes fatigue damage to the road surface equivalent to the passage of 12 standard axles. The results are presented in Table 4.

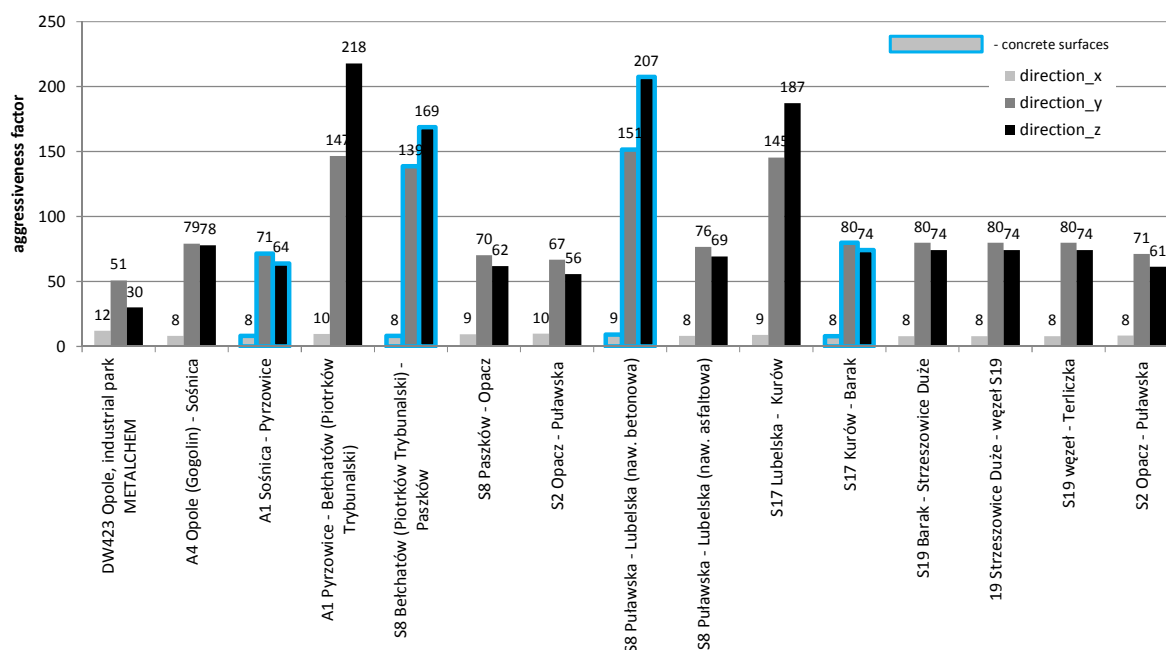
**Tab. 4.** Fatigue damage and aggressiveness factor results

	direction_x	direction_y	direction_z
<b>DW423 Opole, industrial park METALCHEM</b>			
transport set damage sum 1/N	3.07E-06	4.24E-06	7.69E-07
oś 115 kN damage 1/N	2.52E-07	8.34E-08	2.56E-08
aggressiveness factor	<b>12</b>	<b>51</b>	<b>30</b>
<b>A1 Pyrzowice - Bełchatów (Piotrków Trybunalski)</b>			
transport set damage sum 1/N	1.30E-07	8.38E-07	2.58E-08
oś 115 kN damage 1/N	1.36E-08	5.71E-09	1.18E-10
aggressiveness factor	<b>10</b>	<b>147</b>	<b>218</b>

Analyzing the obtained aggressiveness coefficient values (also for other sections not included in the article), it was found that for deformations acting in the X direction, they range from 8 to 12, in the Y direction from 51 to 151, and in the Z direction from 30 to 218. These numbers indicate the number of standard axle passes that cause the same fatigue damage as the passage of a single transport unit. It should be noted that the permissible number of standard axle loads for pavements characterized by the number 218 is approximately 3,000,000,000, so this is a small fraction of the permissible number of loads. Similarly, for pavements characterized by the number 8, the permissible number of loads is approximately 35,000,000. In summary, it should be stated that the aggressiveness of the transport unit relative to the standard axle is insignificant in the case of occasional passage.

### Summary

This study analyzed the impact of a transport unit carrying an oversized load on various pavement structures along its route. Computational models determined strain and stress values, which were used to determine fatigue life. Fatigue life was used to determine the aggressiveness coefficient, which defines the number of standard axles that would cause the same fatigue damage to the pavement as a single transport unit (tractor + trailer + trailer + pusher). Figure 15 summarizes the aggressiveness coefficient values for all analyzed pavements along the route. Concrete pavements are additionally highlighted in blue.



15. Aggressiveness factor results for analyzed pavements

It should be noted that for concrete pavements, the permissible number of standard axle loads is approximately 85,000,000 axles of 115 kN during their service life. For flexible surfaces, the permissible number of standard axle loads is approximately 40,000,000 115 kN axles.

Ultimately, the impact of a transport unit is not significant compared to a standard 115 kN axle. One transport unit run (with a total of 42 axles) corresponds to runs of 8 to 218 standard axles. This is a small fraction of the permissible number of standard axle loads.

### Source materials

- [1] Szydło Antoni „Statyczna identyfikacja parametrów modeli nawierzchni lotniskowych”, Prace Naukowe Instytutu Inżynierii Lądowej Politechniki Wrocławskiej, nr 45/1995
- [2] Katalog typowych konstrukcji nawierzchni sztywnych, GDDKiA, Warszawa, 2014
- [3] Katalog typowych konstrukcji nawierzchni podatnych i półsztywnych, GDDKiA, Warszawa 2014
- [4] FINN F.N., SARAF C., KULKARNI R., NAIR K., SMITH W., ABDULAH A., The use of Distress Prediction Subsystems for the Design of Pavement Structures, Proceedings, Fourth International Conference on the structural Design of Asphalt Pavements, University of Michigan, Ann Arbor, 1977, Vol. 1, 3–38
- [5] Guide for Mechanistic–Empirical Design of New and Rehabilitated Pavement Structures, Final Report, Part 3 – Design and Analysis, NCHRP, TRB, NRC, March 2004
- [6] Applied Research Associates (ARA). 2004. Guide for Mechanistic-Empirical Design of New and Rehabilitated Pavement Structures. Final Report. Transportation Research Board